Ocean Dynamics (2016) 66:367–386
DOI 10.1007/s10236-016-0922-6

Partial ages: diagnosing transport processes by means of multiple clocks

Anne Mouchet[1,2] · Fabien Cornaton[3] · Éric Deleersnijder[4,5] · Éric J. M. Delhez[6]

Received: 4 September 2015 / Accepted: 12 January 2016 / Published online: 9 February 2016

Abstract The concept of age is widely used to quantify the transport rate of tracers - or pollutants - in the environment. The age focuses only on the time taken to reach a given location and disregards other aspects of the path followed by the tracer parcel. To keep track of the subregions visited by the tracer parcel along this path, partial ages are defined as the time spent in the different subregions. Partial ages can be computed in an Eulerian framework in much the same way as the usual age by extending the Constituent oriented Age and Residence Time theory (CART, www.climate.be/CART). In addition to the derivation of theoretical results and properties of partial ages, applications to a 1D model with lateral/transient storage, to the 1D advection-diffusion equation and to the diagnosis of the ventilation of the deep ocean are provided. They demonstrate the versatility of the concept of partial age and the potential new insights that can be gained with it.

Keywords Age · Advection-diffusion · Tracer methods

Responsible Editor: Tal Ezer

✉ Éric J. M. Delhez
e.delhez@ulg.ac.be

[1] Laboratoire des Sciences du Climat et de l'Environnement (LSCE), CEA/CNRS/UVSQ/IPSL, Bât. 701 Orme des Merisiers, 91191 Gif-sur-Yvette Cedex, France

[2] University of Liege (ULg), Astrophysics, Geophysics and Oceanography Department, Sart-Tilman B5c, B-4000 Liège, Belgium

[3] Groundwater Modelling Centre DHI-WASY GmbH, Volmerstraβe 8, 12489 Berlin, Germany

[4] Université catholique de Louvain (UCL), Institute of Mechanics, Materials and Civil Engineering (IMMC) & Earth and Life Institute (ELI), 4 Avenue G. Lemaître, 1348 Louvain-la-Neuve, Belgium

[5] Delft University of Technology, Delft Institute of Applied Mathematics (DIAM), Mekelweg 4, 2628CD Delft, The Netherlands

[6] University of Liege (ULg), Department of Aerospace & Mechanical Engineering, Mathematical Modeling & Methods, Sart-Tilman B37, 4000 Liège, Belgium

1 Introduction

One of the main motivations for the study of geophysical flows — in the deep ocean, coastal regions, or inland waters — is the search for an improved understanding of the transport routes and transport rates of dissolved and suspended substances in the environment. Many different physical processes contribute to this transport over a wide range of spatial scales and time scales, which makes it difficult to describe the dynamics in terms of circulation patterns or, even time dependent, velocity fields. In this context, tracer methods (e.g., Thiele and Sarmiento 1990; England 1995; England and Maier-Reimer 2001; Deleersnijder et al. 2001) are particularly useful and efficient because they directly address the resulting integrated effects of the different processes at stake on the transport of contaminants, nutrients, and other substances. In numerical models, specifically designed artificial tracers can also be defined to isolate and quantify the effects of specific processes. These advantages, together with the (apparent) simplicity of the messages that they convey, explain why

tracer methods have been increasingly used to analyze natural flows and unravel the underlying dynamics.

Tracer methods often proceed with the introduction of characteristic timescales to quantify the transport rates of tracers or of water itself. The seminal papers by Bolin and Rodhe (1973), Zimmerman (1976), and Takeoka (1984) provide clear definitions of many of such timescales including the age, residence time, transit time, and turn-over time.

The concept of age is particularly appealing because of its clear definition (in contrast with other timescales that are often defined in slightly different ways by different authors), its versatility, and the ease with which it can be computed. The age of a water/tracer particle is defined as the time elapsed since a user-defined origin which is hence considered as the "birth" of the particle. In most applications, the origin is chosen as the time at which the particle enters the domain of interest or touches one of its boundaries. Accordingly, the age at any interior point of the domain measures the time taken by the water/tracer particle to reach that point and represents therefore a valuable diagnostic to quantify transport rates.

Basically, the age is a Lagrangian concept. Conceptually, each particle can be considered to be equipped with a clock that starts ticking at the instant of its birth or is reset when a specific event takes place (e.g., when the particle hits the surface of the ocean) and hence records the time elapsed since this origin. The computation of the age is therefore easily implemented in any Lagrangian model (e.g., Chen 2007; Liu et al. 2012; Villa et al. 2015)

Fortunately, the age can also be computed in an Eulerian framework if one takes into account the fact that the water/tracer parcels to be considered according to the underlying continuum hypothesis are made of a collection of water/tracer particles carrying different ages. The full Eulerian description of the age field requires the introduction of a distribution of the ages of these particles. The appropriate framework is therefore five-dimensional, i.e., space $\times$ time $\times$ age (Bolin and Rodhe 1973; Hall and Plumb 1994; Delhez et al. 1999; Ginn 1999; Deleersnijder et al. 2001; Haine and Hall 2002). While special techniques can be used to work in this five-dimensional space (Delhez and Deleersnijder 2002; Cornaton 2012), this complexity is avoided in most Eulerian studies by resorting to the steady state hypothesis (e.g., Holzer and Hall 2000; Khatiwala et al. 2009) or by considering only the mean value of the ages of the particles in a water parcel.

Implicitly following the second approach, Thiele and Sarmiento (1990) and, later, England (1995) and Goode (1996) proposed a differential equation for the mean age of the water and used it to compute ventilation timescales in the global ocean.

In the framework of their Constituent-oriented Age and Residence Time theory (CART, www.climate.be/CART), Delhez et al. (1999) and Deleersnijder et al. (2001) derived a system of two equations allowing for the straightforward computation of the mean age of every seawater constituent, including substances involved in bio-geochemical reactions. The first equation is just the basic transport equation for the constituent, including appropriate reaction terms when necessary. The second is a reaction-transport equation for the so-called age concentration, which is the product of the concentration of the constituent by its mean age. The age concentration is an extensive variable; it satisfies a budget equation that can be used to compute the mean age of the constituent. This approach has been applied in a large number of studies (e.g., Gourgue et al. 2007; Meier 2007; Plus et al. 2009; Bendtsen et al. 2009; de Brye et al. 2012; Bendtsen and Hansen 2013; Ren et al. 2014; Du and Shen 2015).

The concept of age is a very flexible one. In numerical models, different tracers and ages can be defined to focus on specific aspects of the dynamics. For instance, in their study of the dynamics of sediments in the Belgian coastal zone, Mercier and Delhez (2007) define two different ages providing a focus, respectively, on the rate of horizontal transport of the suspended matter and on the time spent by sediment flocs in the water column, i.e., on the frequency of deposition-resuspension events. In de Brye et al. (2012), two different tracers tagging the freshwater entering from the upstream boundary and the water entering from the coastal area are used to compute two water renewal timescales in the Scheldt Estuary.

In the last two applications, different ages are associated with different tracers to study different aspects of a single system. The aim of this paper is to show that different ages can also be attached to a single tracer to provide deeper insights into the dynamics. In the following sections, the concept of partial age will first be introduced and Eulerian equations for partial ages will be derived. Then, applications to a 1D model with lateral/transient storage, to the 1D advection-diffusion equation and to the diagnosis of the ventilation of the deep ocean will be considered.

2 The concept of partial age

As described in Section 1, the age of a particle is the total time elapsed since the birth of this particle, which generally coincides with the time at which the particle entered the domain of interest. Accordingly, the age a of a particle that is located at x at time t measures the time taken by this particle to reach x from the place where it was born at time $t - a$. This explains why the concept of age can be used to quantify transport rates.

With the concept of age, the only information that is available about the path of the particle from its initial location to the observation point x is the total duration of the journey. By doing this, much information is therefore lost about the trajectory of the particle. In particular, all the information about the different subregions visited by the particle during its journey are lost. The concept of partial age that we introduce in this paper aims at making a better use of this information to diagnose transport routes and rates.

To ease the introduction of the concept of partial age, consider the idealized system schematized in Fig. 1 where tracer particles are released by a river discharging into a coastal region with different bays and sub-basins (e.g., Liu et al. 2012). The figure shows the trajectories of two particles released at the same time t_0 and reaching the same offshore location at the observation time $t_\star$. Assuming that the release of the particles in the coastal waters is considered as the birth of these particles, the ages of the two particles at time $t_\star$ are identical and given by the time $t_\star - t_0$ elapsed since they entered the domain of interest through the river outlet. Obviously, the particles have different histories, a fact that is not reflected by the common value of their ages. In order to address the fact that different regions are visited by the two particles, one introduces a partition of the domain of interest ω into a set of (biologically, geographically and/or physically significant) nonoverlapping subregions ω_i, $i \in \{1, \ldots, n\}$, i.e.,

$$\omega = \bigcup_{i=1}^{n} \omega_i, \qquad \forall i \neq j : \omega_i \cap \omega_j = \emptyset \tag{1}$$

and defines the partial age a_i of a particle with respect to a subregion ω_i as the time spent by the particle in this particular subregion (Liu et al. 2012; Deleersnijder et al. 2014). Accordingly, each particle can be characterized by a set of n partial ages $a_1, a_2, \ldots, a_n$ with respect to the n different subregions. In particular, the partial ages, at time $t_\star$, of the particle that immediately turns left after its release (Fig. 1) are given by

$$a_1 = (t_1 - t_0) + (t_3 - t_2), \quad a_2 = (t_2 - t_1), \quad a_3 = (t_4 - t_3), \quad a_4 = (t_\star - t_4) \tag{2}$$

For the second particle, the partial ages are

$$a_1 = (t_1' - t_0), \quad a_2 = 0, \quad a_3 = 0, \quad a_4 = (t_\star - t_1') \tag{3}$$

Obviously, these partial ages can be used to highlight the different histories of the two particles; the additional pieces of information available upon using partial ages can be used to better describe and understand the dynamics of the system under study. In particular, some knowledge of the paths followed by the particles to reach a given region can be used to address connectivity issues.

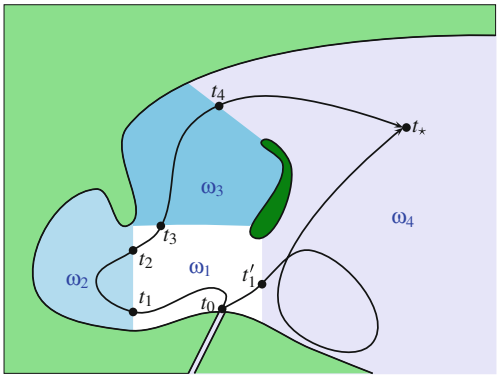

Fig. 1 Schematized picture of a river discharging into a coastal region and of the paths of two particles visiting different subregions. The domain is split into four non overlapping subdomains

From a Lagrangian point of view, the determination of partial ages amounts to equipping each particle with n different watches that are all set to zero at the birth of the particle but with the ith clock ticking only when the particle is in the ith subdomain ω_i. If the different subdomains form a partition of the domain of interest according to Eq. 1, only one clock is ticking at a time (since the subdomains do not overlap) and there is always one clock ticking at any time (since the subdomains form a cover of ω). Therefore, the usual age of a particle is simply the sum of its partial ages, i.e.,

$$a = \sum_{i=1}^{n} a_i \tag{4}$$

The partial ages account for the time spent in the different subdomains ω_i and provide therefore a decomposition of the the total time spent in ω, i.e., the (total) age. This additivity property justifies the name "partial age" coined for $a_1, a_2, \ldots, a_n$.

3 Eulerian equations for partial ages

Partial ages can be easily computed in an Eulerian framework by a straightforward extension of the procedure defined in the Constituent-oriented Age and Residence Time theory (CART) (Deleersnijder et al. 2001).

CART relies on the solution of two coupled equations to compute the mean age of a constituent. The first equation is the usual transport equation for the constituent, i.e.,

$$\frac{\partial C}{\partial t} = \mathcal{L}(C) \tag{5}$$

where

$$\mathcal{L}(\cdot) \equiv \nabla \cdot [\mathrm{K} \cdot \nabla(\cdot) - \mathbf{v}(\cdot)] \tag{6}$$

is the linear advection-diffusion operator, $\mathbf{v}$ is the velocity vector and K is the (supposedly symmetric and positive definite) diffusivity tensor. The second equation is a reaction-transport equation for the so-called age concentration α that can be defined as the product

$$\alpha(t, \mathrm{x}) = C(t, \mathrm{x}) a(t, \mathrm{x}) \tag{7}$$

of the concentration of the constituent by its mean age a. It can be shown that the age concentration is an extensive variable that characterizes the "age content" of a water parcel and satisfies the budget equation (Delhez et al. 1999; Deleersnijder et al. 2001)

$$\frac{\partial \alpha}{\partial t} = C + \mathcal{L}(\alpha) \tag{8}$$

The mean age can thus be computed from Eq. 7 using the solutions of the two coupled Eqs. 5 and 8 with appropriate initial and boundary conditions.

Note that, while the above Eqs. 5 and 8 are expressed here for a passive constituent that is simply transported by the flow, the theory can easily cope with constituents involved in chemical reactions or biological interactions through the introduction of appropriate source/sink terms in Eqs. 5 and 8 (e.g., Delhez et al. 2004).

To understand the origin of Eq. 7 and the modification required to describe partial ages, it is important to realize that the particles located at the same location at a given time have different histories and, hence different ages. To account for this variety, CART relies on the concentration distribution function $c(t, \mathrm{x}, \tau)$ to describe the distribution of the concentration along the age dimension. The concentration distribution function is such that $c(t, \mathrm{x}, \tau) d\tau$ measures the concentration of the material with an age in the range $[\tau, \tau + d\tau]$ so that the (usual) concentration and the mean age are related to c through the equations

$$C(t, \mathrm{x}) = \int_0^\infty c(t, \mathrm{x}, \tau) d\tau \tag{9}$$

and

$$\alpha(t, \mathrm{x}) = \int_0^\infty \tau \; c(t, \mathrm{x}, \tau) d\tau \tag{10}$$

According to Eq. 7, the mean age appears therefore as the normalized first-order moment of the age concentration distribution.

In the same way, a partial age concentration distribution function c_i can be defined such that $c_i(t, \mathrm{x}, \tau) d\tau$ measures the concentration of the material with a partial age a_i in the range $[\tau, \tau + d\tau]$. The partial age concentration distribution functions describe the distributions of the particles present at the same time and location along the partial age dimension so that

$$C(t, \mathrm{x}) = \int_0^\infty c_i(t, \mathrm{x}, \tau) d\tau \quad \forall i \in \{1, \ldots, n\} \tag{11}$$

Equations 9 and 11 show that c and the partial age concentrations c_i each correspond to different decompositions of the concentration C. When using the age concentration c, the different tracer parcels contributing to the concentration C are differentiated by their age. By contrast, the same tracer parcels are sorted out with respect to the time spent in the subdomain ω_i, i.e., their partial age, to build the partial age concentration c_i.

Similarly to Eqs. 7 and 10, mean partial ages can be defined as the normalized first-order moments of the corresponding distributions, i.e.,

$$a_i(t, \mathrm{x}) = \frac{\alpha_i(t, \mathrm{x})}{C(t, \mathrm{x})} \tag{12}$$

where the so-called partial age concentrations α_i are given by

$$\alpha_i(t, \mathrm{x}) = \int_0^\infty \tau \; c_i(t, \mathrm{x}, \tau) d\tau \tag{13}$$

For a passive tracer, the concentration distribution function satisfies the differential equation (Delhez et al. 1999; Deleersnijder et al. 2001)

$$\frac{\partial c}{\partial t} + \frac{\partial c}{\partial \tau} = \mathcal{L}(c) \tag{14}$$

The second term of the left-hand side, the ageing term, can be seen as an advection term acting at a unit velocity along the age dimension; as time goes by, the material tends to get older at the rate of one time unit per elapsed time unit.

A differential equation similar to Eq. 14 can also be easily written. In Eq. 14, the ageing term is active at all time, whatever the location of the particles. For the partial age concentration distribution function c_i, ageing should happen only when the tracer is located in the control domain ω_i. Therefore, the differential equation for the partial age concentration distribution reads

$$\frac{\partial c_i}{\partial t} + \delta_{\omega_i} \frac{\partial c_i}{\partial \tau} = \mathcal{L}(c_i) \tag{15}$$

where

$$\delta_{\omega_i}(\mathrm{x}) = \begin{cases} 1 & \text{if } \mathrm{x} \in \omega_i \\ 0 & \text{if } \mathrm{x} \notin \omega_i \end{cases} \tag{16}$$

is the characteristic function of the subdomain ω_i.

Delhez et al. (1999) and Deleersnijder et al. (2001) showed how the differential Eqs. 5 and 8 for the concentration and for the age concentration can be recovered by integrating (14) over the age dimension. The application

of the same procedure to Eq. 15 leads to the differential equation for α_i, i.e.,

$$\frac{\partial \alpha_i}{\partial t} = \delta_{\omega_i}\, C + \mathcal{L}(\alpha_i) \tag{17}$$

With (5), this equation forms a set of two coupled partial differential equations whose solutions can be used to compute the partial age a_i from Eq. 12. The determination of the full set of partial ages $a_1, a_2, \ldots, a_n$ requires the resolution of (5) together with the n different versions of Eq. 17 corresponding to the n nonoverlapping subdomains ω_i included in the partition of the domain of interest.

Using the linearity of the advection-diffusion operator $\mathcal{L}$, the differential Eq. 8 for the age concentration α can be recovered by summing the n Eq. 17 for the partial age concentrations. Since the Eqs. 8 and 17 are subjected to the same auxiliary conditions, their solutions are such that

$$\alpha = \sum_{i=1}^{n} \alpha_i \tag{18}$$

i.e., the partial age concentrations α_i form a decomposition of the age concentration. The additivity property (4) of the partial ages naturally follows from the definitions Eqs. 10 and 13.

It should be realized that, unlike a and α, the concentration distribution function c cannot be expressed as the sum of the corresponding partial concentration distribution functions c_i, i.e.,

$$c \neq \sum_{i=1}^{n} c_i \tag{19}$$

The distributions of age and partial ages are independent of each other. A simple discrete example can be easily conceived to show that c and the c_i convey different information. Consider two particles $P^{(1)}$ and $P^{(2)}$ of a given tracer and their partial ages $(a_+^{(1)}, a_-^{(1)})$ and $(a_+^{(2)}, a_-^{(2)})$ measuring the time spent in two sub-domains ω_+ and ω_- forming a partition of the whole model domain ω. From the additivity property of partial ages, the (total) ages of the two particles are given by

$$a^{(\beta)} = a_+^{(\beta)} + a_-^{(\beta)}, \qquad \beta \in \{1, 2\} \tag{20}$$

Two hypothetical scenarios for these two particles are envisaged in Table 1.

The distributions of each partial age for the set $P^{(1)} \cup P^{(2)}$ of the two particles are identical in the two scenarios; in both $\mathcal{A}$ and $\mathcal{B}$, the mixtures made on the two particles have exactly one particle with an age $a_+ = 1$ (arbitrary unit), one particle with an age $a_+ = 2$, one particle with an age $a_- = 2$, and one particle with an age $a_- = 3$. This means that the two scenarios cannot be differentiated by their partial age distributions. The (total) age distributions do however differ (while sharing the same mean value); in the first scenario, the ages of the particles are equal to 3 and 5, while they take the common value of 4 in scenario $\mathcal{B}$. Since identical distributions of the partial ages can lead to different distributions of the age, one concludes that, in general, the concentration distribution function c cannot be expressed as a function of the partial concentration distribution function c_i.

4 One-dimensional model with lateral storage

As a first illustration of the use of the concept of partial ages, consider a one-dimensional flow connected with a lateral storage zone as schematized in Fig. 2. Such a model is commonly used in subsurface flow settings where water and tracers can be stored in low-permeability subregions, like aquitards, or to describe the transport of pollutants in rivers when water and materials can be trapped in stagnant water zones like pools, gravel beds, adjacent wetland areas and other hyporheic zones (e.g., Runkel and Chapra 1993; Wagner and Harvey 1997; Kumar and Dalal 2010). In the so-called transient storage models (TSMs) or dead zone models (DZMs), the river is divided into the main flow zone, where downstream advection occurs, and lateral storage zones, which stagnant waters (e.g., Bencala and Walters 1983). The two zones are coupled by diffusion.

In a 1D approach, the transport of a tracer in such a system can be described by the set of coupled equations (integrated over the cross-section)

$$\frac{\partial (A^m C^m)}{\partial t} = -\frac{\partial (Q C^m)}{\partial x} + A^m \beta (C^s - C^m) \tag{21}$$

$$\frac{\partial (A^s C^s)}{\partial t} = -A^m \beta (C^s - C^m) \tag{22}$$

where C^m and C^s denote the concentration in the main channel and in the lateral storage zone, A^m and A^s are the cross-sections of two zones, $Q = A^m U$ is the flow rate

Table 1 Hypothetical age and partial ages (arbitrary units) of two individual particles $P^{(1)}$ and $P^{(2)}$ and mean values of their mixture $P^{(1)} \cup P^{(2)}$ in two scenarios

Scenario $\mathcal{A}$	a_+	a_-	a	Scenario $\mathcal{B}$	a_+	a_-	a
$P^{(1)}$	1	2	3	$P^{(1)}$	2	2	4
$P^{(2)}$	2	3	5	$P^{(2)}$	1	3	4
$P^{(1)} \cup P^{(2)}$	1.5	2.5	4	$P^{(1)} \cup P^{(2)}$	1.5	2.5	4

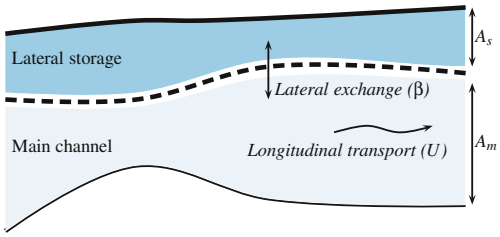

Fig. 2 Channel flow with lateral storage

in the main channel, U is the average velocity in the main channel, and where $\beta > 0$ is a characteristic exchange frequency used to parameterize the mass exchange between the two zones. Since the above model (21)–(22) ignores longitudinal diffusion in both the main channel and the storage zone, the particles can move only downstream and only in the main channel. The time spent in the storage zone reduces therefore the rate of downstream transport. These processes can be quantified using the concept of age. In particular, considering the fate of material entering the main channel at the upstream boundary located at $x = 0$, we define the mean age as the time elapsed since this origin. The corresponding age concentrations in the main channel and the storage zone satisfy

$$\frac{\partial(A^m\alpha^m)}{\partial t} = A^m C^m - \frac{\partial(Q\alpha^m)}{\partial x} + A^m\beta(\alpha^s - \alpha^m) \quad (23)$$

$$\frac{\partial(A^s\alpha^s)}{\partial t} = A^s C^s - A^m\beta(\alpha^s - \alpha^m) \quad (24)$$

where the first term on the right-hand-side accounts for the ageing process. The mean age can be obtained by integrating forward in time the Eqs. 21–24 from homogenous initial conditions subject to the boundary conditions

$$C^m(t,0) = 1, \quad \alpha^m(t,0) = 0 \qquad \forall t \quad (25)$$

and taking the ratios

$$a^m = \frac{\alpha^m}{C^m}, \qquad a^s = \frac{\alpha^s}{C^s} \quad (26)$$

It is noteworthy that Eqs. 22 and (24) do not contain spatial derivatives and, therefore, do not require any boundary condition.

If the cross-sectional areas and the different parameters are assumed to be constant and uniform, the velocity U itself is a constant and the system evolves toward a steady solution characterized by a uniform concentration field. The corresponding mean ages in the different sub-domains can then be expressed in closed form, i.e.,

$$a^m(x) = (1+\gamma)\frac{x}{U} \quad (27)$$

and

$$a^s(x) = (1+\gamma)\frac{x}{U} + \frac{\gamma}{\beta} \quad (28)$$

where $\gamma = A^s/A^m$. These results show that the net downstream transport rate is decreased by a factor $1/(1+\gamma)$ with respect to a river system without lateral storage zone. The age distributions (27)–(28) are not very intuitive. While they are clearly useful to study the dynamics of processes occurring at the same rate in both the main stream and the lateral storage zone (e.g., radioactive decay of a tracer, organisms growing at the same rate regardless of location), these timescales are not appropriate to deal with processes with different dynamics in the two subsystems (e.g., larger photobleaching in the shallow stagnant water zones) and do not really help to understand and quantify the dynamics of the exchange between the main stream and the lateral storage zone.

New insights can be brought by the introduction of two partial ages measuring, respectively, the time spent in the main channel and in the lateral storage zone. More precisely, four variables a_ξ^η with $\xi, \eta \in \{m, s\}$ can be defined where the subscript refers to the sub-domain with respect to which the partial age is computed and the superscript points to the zone where the variable is defined. Accordingly, a_s^m, for instance, describes the distribution in the main channel of the partial age with respect to the storage zone.

In accordance with the additivity property of partial ages (4), the mean ages can be split into their partial age components as

$$a^m = a_m^m + a_s^m \quad (29)$$

and

$$a^s = a_m^s + a_s^s \quad (30)$$

Because longitudinal transport occurs only in the main channel, the distance x traveled by a particle downstream the upper boundary is a direct measure of the time spent in the main channel, i.e., of its partial age with respect to the main channel. More precisely, one has

$$a_m^m(x) = a_m^s(x) = \frac{x}{U} \quad (31)$$

In Eqs. 21–22, the exchange process between the main channel and the storage zone is parameterized in an Eulerian way as a first-order process. This process controls the ratio of the times spent by a particle in the two subregions. As far as this ratio is concerned, longitudinal advection can be ignored since the parameters of the model do not depend on the longitudinal coordinate x.

The exchange process can then be described in a Lagrangian way by considering that any particle located in the main channel has a given probability p_m to move to the storage zone during a given time interval dt while a particle located in the storage zone has a probability p_s of taking the reverse course in the same time interval. Since the two associated mass fluxes balance each other, the two probabilities p_m and p_s must be inversely proportional to, respectively,

A_m and A_s. As a consequence, the times spent in the two zones, i.e., the partial ages, of the particles found in the main channel are proportional to these cross-sections, i.e.,

$$\frac{a_s^m(x)}{a_m^m(x)} = \frac{A_s}{A_m} = \gamma \tag{32}$$

Therefore,

$$a_s^m(x) = \gamma\ a_m^m(x) = \gamma\ \frac{x}{U} \tag{33}$$

The steady state age (27) in the main channel can be recovered by combining Eqs. 31 and (33) with the additivity property (29).

Taking the difference between the total age a^s in the storage zone given by Eq. 28 and the partial age a_m^s as given by Eq. 31, one gets

$$a_s^s = a^s - a_m^s = \gamma \frac{x}{U} + \frac{\gamma}{\beta} = a_s^m + \frac{\gamma}{\beta} \tag{34}$$

While Eqs. 27–(28) merely show that the mean age in the lateral storage zone exceeds the mean age in the main channel at the same location by the constant value γ/β, (34) attributes this constant difference to the time spent in the storage zone; if the mean ages differ, it is because the particles found in the storage zone spend a longer time in this storage zone than what the particles found in the main channel do on average.

It is quite remarkable that the concept of partial age helps to better understand the net downstream rate of the material and the interaction between the longitudinal advection in the main channel and the diffusion like exchange with the storage zone. Better insight can be gained by simple arguments, without solving detailed equations.

The above results about partial ages can also be obtained mathematically by calculating the ratios

$$a_\xi^\eta(t,x) = \frac{\alpha_\xi^\eta(t,x)}{C^\eta(t,x)} \qquad \text{with} \qquad \xi,\eta \in \{m,s\} \tag{35}$$

where the partial age concentrations α_ξ^η satisfy the differential equations

$$\frac{\partial(A^m\alpha_m^m)}{\partial t} = A^m C^m - \frac{\partial(Q\alpha_m^m)}{\partial x} + A^m\beta(\alpha_m^s - \alpha_m^m) \tag{36}$$

$$\frac{\partial(A^s\alpha_m^s)}{\partial t} = -A^m\beta(\alpha_m^s - \alpha_m^m) \tag{37}$$

$$\frac{\partial(A^m\alpha_s^m)}{\partial t} = -\frac{\partial(Q\alpha_s^m)}{\partial x} + A^m\beta(\alpha_s^s - \alpha_s^m) \tag{38}$$

$$\frac{\partial(A^s\alpha_s^s)}{\partial t} = A^s C^s - A^m\beta(\alpha_s^s - \alpha_s^m) \tag{39}$$

and the boundary conditions

$$\alpha_m^m(t,0) = \alpha_s^m(t,0) = 0 \qquad \forall t \tag{40}$$

These equations are easily obtained by integrating (17) over the cross-sections of the main channel and the storage zone. Their right-hand sides reflect the fact that the clock used to define the partial ages a_m^m and a_m^s measuring the time spent in the main channel is ticking only for the particles located in the main channel while, when computing a_s^m, a_s^s and the related partial age concentrations α_s^m and α_s^s, ageing is taken into account only in the storage zone.

The Eqs. 21, 22, and 36–39, together with the corresponding initial and boundary conditions can be used to compute the transient solution.

At a steady state, the concentration field is uniform, with a unit concentration in both the main channel and the storage zone. The distributions (31), (33), and (34) of the partial ages derived above from physical arguments can then be easily recovered as steady-state solutions of Eqs. 36–(39).

The above equations can also easily be adapted to take into account longitudinal diffusion processes and diagnose the longitudinal transport in more realistic versions of this dead zone model.

5 Partial ages in a 1D advection-diffusion model

As a second illustration of the concept of partial age, consider the transport of a passive tracer that is released at a constant rate J at the origin $x = 0$ of the infinite one-dimensional domain $x \in]-\infty, +\infty[$ in which the velocity u and Laplacian diffusion coefficient $\kappa > 0$ are constant and uniform. Without loss of generality, we assume that $u > 0$.

The tracer concentration obeys

$$\frac{\partial C}{\partial t} + u\frac{\partial C}{\partial c} = J\delta(x) + \kappa\frac{\partial^2 C}{\partial x^2} \tag{41}$$

where δ denotes the Dirac generalized function. If the age of the tracer is defined as the time elapsed since its release into the system through the point source, the corresponding age concentration is given by

$$\frac{\partial \alpha}{\partial t} + u\frac{\partial \alpha}{\partial x} = C + \kappa\frac{\partial^2 \alpha}{\partial x^2} \tag{42}$$

The concentration tends then to the steady state distribution

$$C^\infty(x) = \begin{cases} \dfrac{J}{u} & x \geq 0 \\ \dfrac{J}{u}\mathrm{e}^{ux/\kappa} & x < 0 \end{cases} \tag{43}$$

while the steady state age distribution can be described as

$$a^\infty(x) = \frac{\alpha^\infty(x)}{C^\infty(x)} = \frac{|x|}{u} + \frac{2\kappa}{u^2} \tag{44}$$

Quite surprisingly, the age is symmetric about the origin despite the dissymmetry introduced by the onedirectional flow. In other words, tracer parcels, whether located upstream or downstream from the point source, show exactly the same mean age if they are located at the same

distance from the source. This rather counterintuitive property is further studied in Deleersnijder et al. (2001), Beckers et al. (2001), and Deleersnijder and Delhez (2004). Hall and Haine (2004) provide also an elegant Lagrangian explanation in a slightly different context.

The concept of partial age can be used to get deeper insight into the transport mechanisms. To this end, the domain of interest is split into the two nonoverlapping subdomains

$$\omega_- =]-\infty, 0[, \qquad \omega_+ =]0, +\infty[\tag{45}$$

The corresponding partial age concentrations can be obtained as the solutions of

$$\frac{\partial \alpha_\pm}{\partial t} + u\frac{\partial \alpha_\pm}{\partial x} = \delta_{\omega_\pm} C + \kappa \frac{\partial^2 \alpha_\pm}{\partial x^2} \tag{46}$$

At steady state, one gets

$$\alpha_+^\infty(x) = \begin{cases} \dfrac{J(ux+\kappa)}{u^3} & x \geq 0 \\ \dfrac{J\kappa}{u^3} e^{ux/\kappa} & x < 0 \end{cases} \tag{47}$$

and

$$\alpha_-^\infty(x) = \begin{cases} \dfrac{J\kappa}{u^3} & x \geq 0 \\ \dfrac{J(u|x|+\kappa)}{u^3} e^{ux/\kappa} & x < 0 \end{cases} \tag{48}$$

Therefore, the mean partial ages are given by

$$a_+^\infty = \begin{cases} \dfrac{x}{u} + \dfrac{\kappa}{u^2} & x \geq 0 \\ \dfrac{\kappa}{u^2} & x < 0 \end{cases} \tag{49}$$

and

$$a_-^\infty = \begin{cases} \dfrac{\kappa}{u^2} & x \geq 0 \\ \dfrac{|x|}{u} + \dfrac{\kappa}{u^2} & x < 0 \end{cases} \tag{50}$$

One can easily check that

$$a^\infty = a_-^\infty + a_+^\infty \tag{51}$$

The different ages are plotted in Fig. 3.

Note that the partial age concentration distribution function c_i for this 1D advection-diffusion problem can also be computed explicitly (Deleersnijder 2015). The results illustrate the fact that, as explained in Section 3, there is no relation between CART's classical age distribution functions and the partial age distribution functions.

In the mean, tracer particles found at the origin have spent an equal amount of time in the upstream and downstream halfs of the domain, i.e.,

$$a_+^\infty(0) = a_-^\infty(0) = \frac{\kappa}{u^2} = \frac{a^\infty(0)}{2} \tag{52}$$

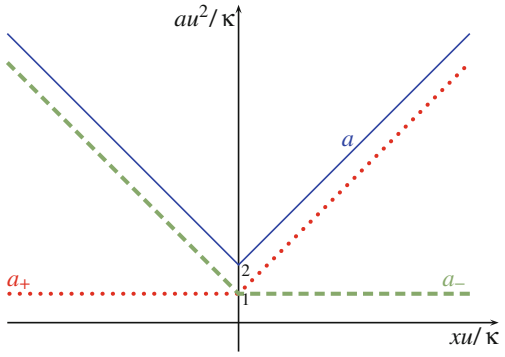

Fig. 3 Age and partial ages at steady state in a one-dimensional flow

Not unexpectedly, the values of the two partial ages (and of the total age) decrease with u, since a large mean velocity tends to flush older material away from the origin and increases with κ, since diffusion helps to bring older particles back to the origin.

The fact that the two partial ages are equal at the origin might come as a surprise. This result can, however, be explained by resorting to Lagrangian arguments. To this end, note that the advection-diffusion dynamics can be described as the continuous limit of a discrete random walk of particles on an infinite 1D lattice. Let p_+ be the probability for a positive step and $p_- = 1 - p_+$ the probability for a negative step, where all steps have the same length Δx and occur at the constant time interval Δt. All the particles that can be found at the origin have either been just released (their age and partial ages are zero) or have returned to the origin after a $2n$-step path made of exactly n positive steps and n negative steps. To each $2n$-step path, one can associate a mirror path obtained by reversing the direction of its $2n$ constitutive steps. The particles following the original path and the mirror path share the same (total) age $2n\Delta t$ but have complementary partial ages in the sense that the partial age a_+ (resp. a_-) of the particle along the original path is equal to the partial age a_- (resp. a_+) of the particle along the mirror path since, at any time, the second particle is located at $-x$ when the first particle is at $+x$. Because they contain the same number of (independent) positive and negative steps, the original path and its mirror path have the same probability

$$\mathcal{P}_{n,n} = p_+^n p_-^n \tag{53}$$

so that the number of particles following the two paths are equal. Therefore, the particles following a path and the associated mirror path, when considered together, bring identical contributions to the two partial ages at the origin. In other words, the partial age concentration distribution function c_- and c_+ are identical at the origin and so are their mean values a_- and a_+.

Unlike the age itself, partial ages are not symmetric with respect to the origin (or at least not in the same sense as the

mean age, see below). The particles that are found in the downstream (resp. upstream) subdomain have spent a larger proportion of their life in the downstream (resp. upstream) half of the domain. This fact is quantified by the two partial ages a_- and a_+ and forms the added value of partial ages.

The spatial distributions of the two partial ages can be easily explained. The paths of a particle from the origin to a location $x^\star > 0$ can be split into two subpaths. The first subpath form a closed loop around the origin. The second subpath is entirely included in ω_+ and goes directly from the origin to the final location $x^\star$. During the first subpath, the particle gains both partial ages a_+ and a_-. From the above reasoning about partial ages at the origin, it is clear that the two partial ages acquired during this first subpath are equal: at steady state, according to Eq. 52, the contributions to two mean partial ages are given by

$$a_+^1 = a_-^1 = \frac{\kappa}{u^2} \tag{54}$$

During the second subpath, the particle does not leave ω_+ so that the contribution a_-^2 to partial age a_- is zero, i.e., a_- remains then constant. The mean partial age a_+^2 gained during this second phase is equal to the time $x^\star/u$ taken to travel from the origin to $x^\star > 0$. The results (49)–(50) can then be recovered by summing the contributions of the two subpaths to the partial ages, i.e.,

$$a_\pm = a_\pm^1 + a_\pm^2 \tag{55}$$

The mean partial age $a_+^2 = x^\star/u$ associated with the second subpath requires an explanation. Obviously, the result is correct if $\kappa = 0$. However, the result remains correct even when diffusion cannot be ignored. Diffusion does induce the spreading of the distribution of partial ages but does not modify the mean. The partial age a_+^2 associated with this second subpath is the usual (total mean) age a_0 of a tracer or a water parcel when the age is defined as the time elapsed since touching the origin for the last time. In this particular framework, the age is computed by considering a tracer with a unit concentration at $x = 0$ — which tags water parcels as they touch the origin — and by prescribing the age to be zero at this location. This set up amounts to resetting the clock attached to the tracer particles every time they touch the origin. Therefore, the age computed in this way appears at the partial age a_+^2 associated with the second subpath considered above. As the age a_0 was previously shown to be independent of the diffusion coefficient (e.g., Deleersnijder et al. 2001; Hall and Haine 2004), a_+^2 shows the same property.

While the partial ages, unlike the total age, are not individually symmetric with respect to $x = 0$, they are symmetric to each other, i.e.,

$$a_-^\infty(x) = a_+^\infty(-x) \tag{56}$$

This property, which generalizes (52), is also valid at any particular time, not only at steady state. It can be explained by resorting to similar Lagrangian arguments as above. The detailed proof can be found in Appendix B. The basic ingredient of the proof is that their are equal numbers of N-step paths from the origin to any location $x^\star = m\Delta x$ and to its mirror point $-x^\star$. The corresponding paths are mirror images of each other so that the increase of the partial age a_+ (resp. a_-) along a path is identical to the increase of the partial age a_- (resp. a_+) along the associated mirror path. Of course, the number of particles following a path and its mirror path differ, which leads to the asymmetry of the concentration field, but the probabilities of the two paths differ by a ratio $(p_+/p_-)^m$. Since this ratio depends only on the location under consideration—and not on the number of steps of the path—it cancels out when computing mean partial ages at any specific location or time. The mean partial ages induced by a continuous release are therefore symmetric to each other at all times.

The above discussion brings to light an other interesting feature of partial ages. By definition, all the N-step paths taken by particles released at $x = 0$ are characterized by the same (total) age $N\Delta t$, whatever the end point of the path. The partial ages do, however, differ for, even if the particles spent the same amount of time in the domain of interest, the time spent in the different sub-domains vary with the end point. As a result, the concept of partial age can be used to characterize transport rates even when the usual age concept is useless. In particular, while the description of the age field of a tracer/pollutant released instantaneously in an accident like event does not convey any useful information — the age is just the time elapsed since the accident — partial ages may still be of use.

6 Diagnosis of the ventilation of the deep ocean

In the World Ocean, it is customary to have recourse to the concept of age to quantify the rate at which deep waters are replaced with water originating from the surface layer (e.g., England 1995; Holzer and Hall 2000; Primeau 2005). This ventilation timescale provides valuable information about the rate at which atmospheric signals/gases propagate into the ocean interior. In this context, the age of a water parcel can be defined as the time elapsed since its last contact with the ocean's surface.

Since the aim is to quantify the rate at which water parcels that touched the ocean surface are transported into deeper layer, a virtual tracer can be introduced to tag the corresponding water mass that forms at the surface. The propagation of this surface water into the ocean's interior can be described by integrating forward in time (5)–(8)

from appropriate initial conditions and with the boundary conditions

$$C(t, \mathrm{x}_s) = 1, \qquad \alpha(t, \mathrm{x}_s) = 0 \qquad \forall \mathrm{x}_s \in \Gamma_s \tag{57}$$

on the ocean's surface Γ_s. The boundary conditions on the age concentration α reflect the fact that the age is defined to be zero at the surface; the virtual clock attached to each parcel of the virtual tracer starts ticking when the parcel leaves the surface and is reset to zero every time it hits the surface again.

As time progresses, the virtual tracer completely fills the whole ocean and its concentration tends to unity everywhere, meaning that all the parcels hit the surface at some previous time. According to Eq. 7, the age concentration is then equal to the age itself and Eq. 8 becomes

$$\frac{\partial a}{\partial t} = 1 + \mathcal{L}(a) \tag{58}$$

The solution of (58) with the boundary condition

$$a(t, \mathrm{x}_s) = 0 \qquad \forall \mathrm{x}_s \in \Gamma_s \tag{59}$$

provides therefore a direct access to the mean age. In most studies on ventilation timescales, only the steady state version of this equation is considered (Deleersnijder et al. 2002).

The boundary conditions Eqs. 57 and 59 are widely used to quantify the ventilation rate of the ocean (e.g., England 1995; Haine and Hall 2002; Deleersnijder et al. 2002). In practice, the modeling results may, however, be strongly dependent on the thickness of the surface layer and other boundary conditions can be considered (e.g., Khatiwala et al. 2009; DeVries and Primeau 2010).

The concept of partial ages can easily be applied in this context by considering the same virtual tracer as for the usual age. Taking into account the fact that this tracer ultimately fills the whole domain, the differential equation for the partial age a_i relative to a subdomain ω_i can be obtained from Eq. 17 and expressed as

$$\frac{\partial a_i}{\partial t} = \delta_{\omega_i} + \mathcal{L}(a_i) \tag{60}$$

This equation must be solved subject to the boundary condition

$$a_i(t, \mathrm{x}_s) = 0 \qquad \forall t \tag{61}$$

at the surface. Partial ages a_i computed in this way have the meaning of the time spent by the water parcels in the sub-domain ω_i since their last contact with the surface. By considering multiple subdomains ω_i, the corresponding partial ages provide new insights into the paths of the water parcels from the surface to the ocean's interior by keeping track of the time spent by water parcels in the different subdomains.

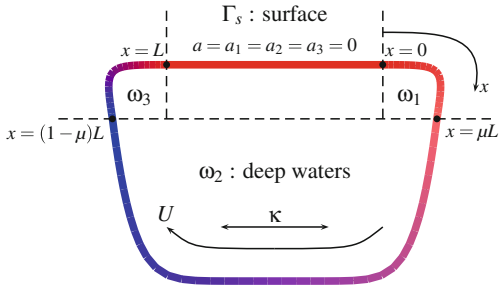

Fig. 4 Schematized model of the ventilation of the World Ocean

A first model describing the transport of the atmospheric signal into the ocean interior can be obtained by twisting the 1D model considered in the previous section into a loop as schematized in Fig. 4. The model is used here as a crude approximation of the global ocean conveyor belt (e.g., Munk 1966; Shaffer and Sarmiento 1995). Water parcels are assumed to leave the surface at $x = 0$ (where x is the curvilinear coordinate along the 1D path) and sink in a sub-region ω_1 to reach the deeper layers ω_2 at $x = \mu L$, where L is the total length of the path below the surface. Water parcels get back to the surface at $x = L$ through the upwelling region ω_3. The transport along the loop is characterized by constant and uniform velocity u and longitudinal diffusion coefficient κ.

The three sub-regions ω_1, ω_2, and ω_3 define a partition of the ocean's interior $[0, L]$. They can be used to define the corresponding partial ages a_1, a_2, and a_3 such that

$$a(x) = a_1(x) + a_2(x) + a_3(x) \tag{62}$$

where a is the (total) mean age, i.e., the time spent since leaving the surface at $x = 0$ or $x = L$. The distributions of these ages can be obtained by solving the appropriate steady-state forms of Eq. 58 and 60 where

$$\mathcal{L} = \kappa \frac{d^2}{dx^2} - u \frac{d}{dx} \tag{63}$$

with the boundary conditions

$$a(0) = a_1(0) = a_2(0) = a_3(0) = 0 \tag{64}$$

and

$$a(L) = a_1(L) = a_2(L) = a_3(L) = 0 \tag{65}$$

The solutions are shown in Fig. 5 for $\mu = 0.2$ and

$$Pe = \frac{uL}{\kappa} = 10 \tag{66}$$

where Pe is the Peclet number. Analytical solutions are provided in Appendix C.

As expected, the age increases downstream from the surface and reaches a maximum in the deeper layer. As the surface is approached again through the upwelling region ω_3, the age decreases toward zero as a result of the diffusive

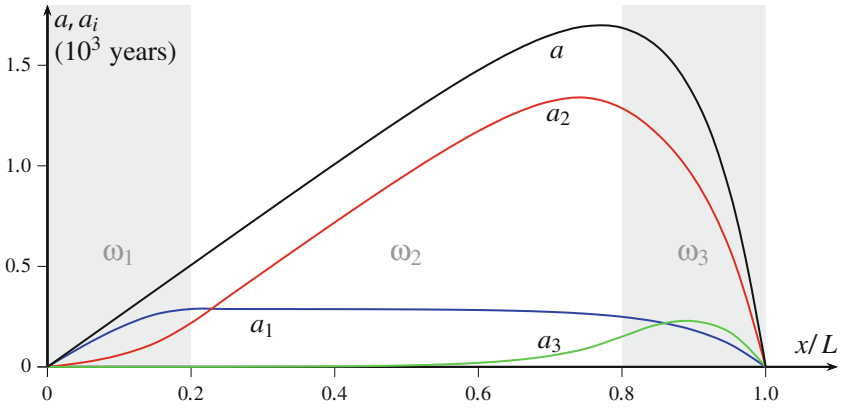

Fig. 5 Steady state distribution of the age and partial ages (unit = 10^3 years) in the model schematized in Fig. 4 for $\mu = 0.2$, $L = 4000$ km, $u = 0.5\ 10^{-7}$ m/s, and $\kappa = 0.2$ cm^2/s corresponding to $Pe = 10$

transport of young water parcels from the surface into the ocean's interior, i.e., against the (upward) mean flow.

Partial ages help to understand the composition of the water masses in the downwelling region ω_1 and the interaction of the advection and diffusion processes. In the largest part of ω_1, the main contribution to the age is from the partial age a_1, i.e., the water parcels found in ω_1 spent most of their life in ω_1. In the vicinity of the downstream boundary of ω_1, however, a_2 contributes significantly to the mean age a. This reflects the upward diffusion of older material from ω_2 into ω_1. The water at the bottom of the downwelling region is a mixture of young water parcels recently advected from the surface and older water parcels having spent a significant amount of time in the deep region ω_3. Using the analytical solutions provided in Appendix C, one can show that

$$a_2(\mu L) \sim \frac{\kappa}{u^2}, \qquad (Pe \to \infty) \tag{67}$$

which confirms that this contribution vanishes when diffusion is small, i.e., when the mechanism of upstream transport is inefficient/disabled.

The spatial distribution of a_1 reflects the dynamics of this partial age. The partial age of a water parcel increases only when the water parcel is in the control domain with respect to which it is defined. As a result, the partial age a_1 of a water parcel reaches its maximum value when leaving ω_1 and remains constant when it is outside ω_1, unless it touches the surface where all ages are reset to zero. This explains why a_1 increases from its initial value of zero at the surface to larger values downwstream and reaches a maximum at the interior boundary $x = \mu L$ between ω_1 and ω_2. In the largest part of ω_2, the partial age a_1 takes a constant value which quantifies the (mean) time spent by the water parcels in ω_1 along their journey to the deep layer. In this region, the main contribution to the age a comes from the partial age a_2, which increases downstream almost everywhere in ω_2.

The partial age a_3 measures the time spent in ω_3. This time is negligible for the particles found in ω_1 and in most parts of ω_2. The main contribution to the age of the water parcels in ω_3 comes from the time spent in ω_2 while a_1 and a_3 have similar contributions.

The decrease of a_1 and a_2 observed as the upwelling region and the surface are approached can be explained in the same way as the decrease of the age itself: it is due to the diffusion of younger water parcels from the surface. This process is also responsible for the occurrence of the maximum value of a_2 in the interior of ω_2 and not on its boundary, as could be expected from the discussion above. Figure 5 shows that a_3 also takes its maximum value around $x = 0.9L$ and not on the boundary of ω_3. The reason for these apparently conflicting results lies in the fact that the partial ages a_1, a_2, and a_3 are only the mean values of the corresponding distributions of the partial ages of the water parcels that make up the fluid. While the partial age a_i of each water parcel does reach its maximum value on the boundary of ω_i, the mean value of the corresponding distribution will not necessarily do so; the location of the possible maximum of the mean partial age of a collection of a water parcels depends on the composition of this collection and is therefore influenced by the diffusive exchange of water parcels with different properties. In Appendix D, we show however that, the absolute maximum of the steady state distribution of a partial age a_i is always achieved in the corresponding region ω_i, but not necessarily on the boundary.

As pointed out by Gnanadesikan et al. (2007), some peculiar behavior can be observed when Pe is small: reducing the velocity does not necessarily increase the age everywhere. Figure 6 shows the spatial distribution of the age and partial ages for two different values of u corresponding to $Pe = 4$ and $Pe = 2$. While, as expected, the age increases in regions ω_1 and ω_2 when u decreases, it decreases in region ω_3. This occurs because, when advection decreases, the age in the upwelling region is more dominated by the diffusion of young water from the surface than by the advection of older water masses from the ocean's interior. As a result, the decrease of the overall rate of ventilation in the

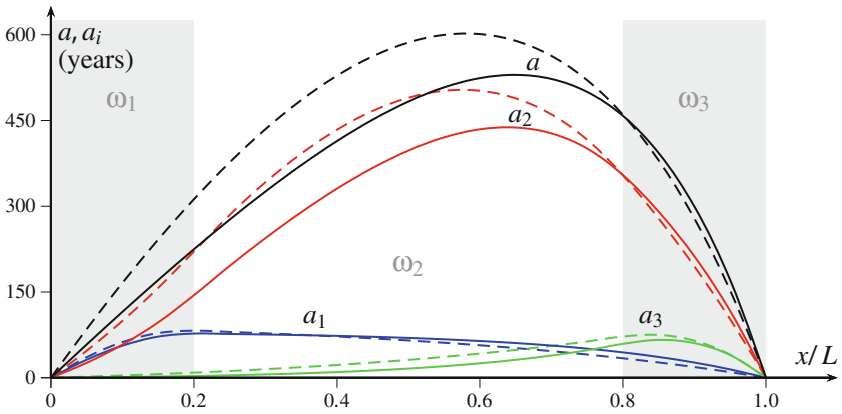

Fig. 6 Steady state distribution of the age and partial ages (in years) in the model schematized in Fig. 4 for $\mu = 0.2$, $L = 4000$ km, $\kappa = 0.2$ cm^2/ with $u = 10^{-7}$ m/s ($Pe = 4$, *solid lines*) and $u = 0.5\ 10^{-7}$ m/s ($Pe = 2$, *dashed lines*)

ocean's interior is compatible with a decrease of the age in the upper water column (Gnanadesikan et al. 2007).

The two partial ages a_1 and a_2 exhibit the same somewhat counterintuitive behavior as the mean age a: in the upwelling region, they decrease with the advection velocity when Pe is small (Fig. 6). However, the partial age a_3 increases everywhere when u is reduced. The different behaviors of the partial ages can be partly explained by the different effects of advection on the three partial ages. As mentioned above, the maximum value of a_1 occurs somewhere in ω_1. When u decreases, a_1 increases slightly in ω_1, as expected, but the net downstream advective flux of this older material to ω_2 and ω_3 decreases. The relative influence of the diffusion flux of the younger material originating from the upwelling region a_3 increases, which tends to decrease a_1 in ω_2 and ω_3. A similar reasoning can be elaborated to explain the observed distribution of a_2 downstream ω_2. The dynamics of a_3 is somewhat different; since the maximum of a_3 occurs in ω_3, the advection flux into ω_3 tends to reduce a_3 in this region. When u decreases, this flux of younger (with respect to a_3) material weakens, and a_3 increases in spite of the larger influence of the diffusion flux of younger surface waters.

Figure 6 shows that the decrease of the mean age observed in region ω_3 when u decreases and Pe is small can be attributed to the decrease of both a_1 and a_2, which is not compensated for by a sufficient increase of a_3. In other words, the particles do not spend less time in ω_3 when the velocity decreases, on the contrary, but the older particles which have build their age in the upstream regions ω_1 and ω_2 are more effectively transported to the surface by diffusion.

While the model schematized in Fig. 4 provides a first general description of the ventilation process in the World Ocean, it is of course not sufficient to capture the complex physics of the real system. In order to demonstrate the applicability of the concept of partial age in a more realistic model, we diagnose here the annual mean

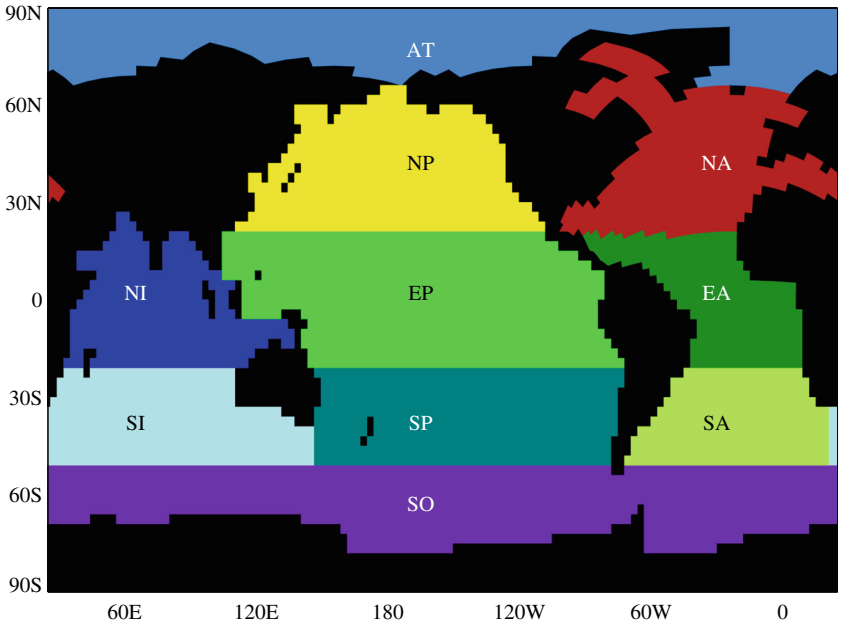

Fig. 7 Horizontal partitioning of the World Ocean in subbasins. Three subdomains are associated to every horizontal box corresponding, respectively, to surface waters (depth between 0 and 500 m), intermediate waters (depth between 500 and 1500 m) and deep waters (depth below 1500 m)

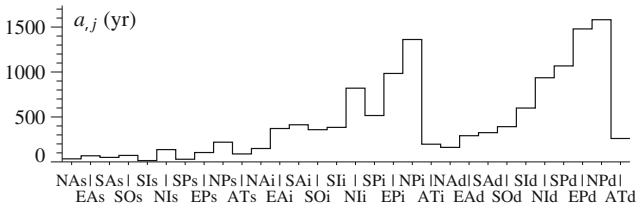

Fig. 8 Mean age $a_{,j}$ in the different sub-basins of the World Ocean

circulation obtained with the 3D Louvain-la-Neuve OGCM (Deleersnijder and Campin 1995; Campin et al. 1999; Campin and Goosse 1999). The latter is a primitive-equation, free-surface OGCM resting on the usual set of assumptions, that is, the hydrostatic and Boussinesq approximations. Detailed descriptions of the model can be found in the above-mentioned references.

In this 3D model, we introduce the partitioning of the World Ocean schematized in Fig. 7. The ocean is first split into ten horizontal sub-basins (AT = Arctic Ocean, NP/EP/SP = Northern, Equatorial and Southern Pacific Ocean, NA/EA/SA = Northern, Equatorial, and Southern Atlantic Ocean, NI/SI = Northern and Southern Indian Ocean, SO = Southern Ocean). Subdomains are formed by splitting each of the sub-basins into a surface box ("s" subscript, depth between 0 and 500 m), an intermediate box ("i" subscript, depth between 500 and 1500 m) and a deep box ("d" subscript, below 1500 m).

The mean values

$$a_{,j} = \frac{1}{V(\omega_j)} \iiint_{\omega_j} a(\mathrm{x}) d\mathrm{x} \tag{68}$$

(where $V(\omega_j)$ is the volume of ω_j) of the age of the water in the different subdomains are shown in Fig. 8. As expected from its definition, the age is maximum in the deeper boxes. By comparison, the age takes very small values in the surface sub-domains since these are relatively shallow and are directly exposed to the surface input. In accordance with the usual understanding of the global circulation, the oldest water masses are found in the Northern Pacific (e.g., England 1995).

The 30 different sub-basins (with surface, intermediate, and deep boxes) defined by Fig. 7 can be used to define 30 different partial ages which can be computed by solving the corresponding versions of Eq. 60. The results can be conveniently presented in matrix form by first averaging the different partial ages on the different sub-domains themselves and forming the partial ages matrix A with elements

$$a_{i,j} = \frac{1}{V(\omega_j)} \iiint_{\omega_j} a_i(\mathrm{x}) d\mathrm{x} \tag{69}$$

where $a_{i,j}$ denotes the mean value over the subdomain ω_j of the partial age a_i with respect to the subdomain ω_i. In other words, $a_{i,j}$ is the mean time spent in ω_i by the water parcels present in ω_j during their journey from the ocean's surface.

Since the 30 subdomains form a complete partition of the World Ocean in non-overlapping subdomains, the corresponding partial ages a_i provide a decomposition of the total age of the water parcels such that the additivity property (4) holds. The subdomain-averaged ages shown in Fig. 8 are related to the subdomain-averaged partial ages through the similar relation

$$a_{,j} = \sum_i a_{i,j} \tag{70}$$

Figure 9 shows the partial ages computed using the OGCM model. In subfigure a, the domain-averaged partial ages $a_{i,j}$ are normalized by the overall average $\bar{a}$ of the age of the water in the World Ocean, i.e., 754 years. In Fig. 9b, the partial ages are normalized by the average age $a_{,j}$ of the water in the corresponding sub-domain. Since the additive property (70) holds, these ratios $a_{i,j}/a_{,j}$ give the relative contributions of the different partial ages to the (total) age $a_{,j}$ in the sub-domain ω_j.

Partial ages help to keep track of the paths followed by the water parcels found in the deeper layers of the Pacific. Figure 9 shows that the water parcels gain their age by transiting for a significant amount of time in the deeper layers of the Equatorial and Southern Pacific and, to a lesser extent, in the intermediate layer of the Northern Pacific and in the deep layers of the Northern Atlantic, Southern Atlantic, and Southern Ocean. About 40 % of the age of the deep Northern Pacific water is, however, due to the time spent in the deep Northern Pacific itself.

Similarly, the age of the water in the deeper layers of the Northern Atlantic can be mostly explained by the time spent by the water parcels in the very same region with small contributions from the time spent in the overlying intermediate waters and in the deeper parts of the Equatorial and Southern Atlantic.

The small ages value found in surface layers can be analyzed using Fig. 9b.

Most of the water parcels are rather young, i.e., they hit the surface only a short time ago. However, surface water masses also include older material from intermediate and deeper layer. Even if the proportion of these water parcels is rather low, they have a significant influence on the mean age because their ages can be very large. For instance, the age of the water in the surface layer of the Northern Pacific can be ascribed to the contribution from the old intermediate Pacific waters and, even more, from the long time spent in the deeper layers by some water parcels.

A detailed analysis of the results shown in Fig. 9 is beyond the scope of this paper. Obviously, however, the short discussion above shows that partial ages provide interesting information for diagnosing the ventilation process

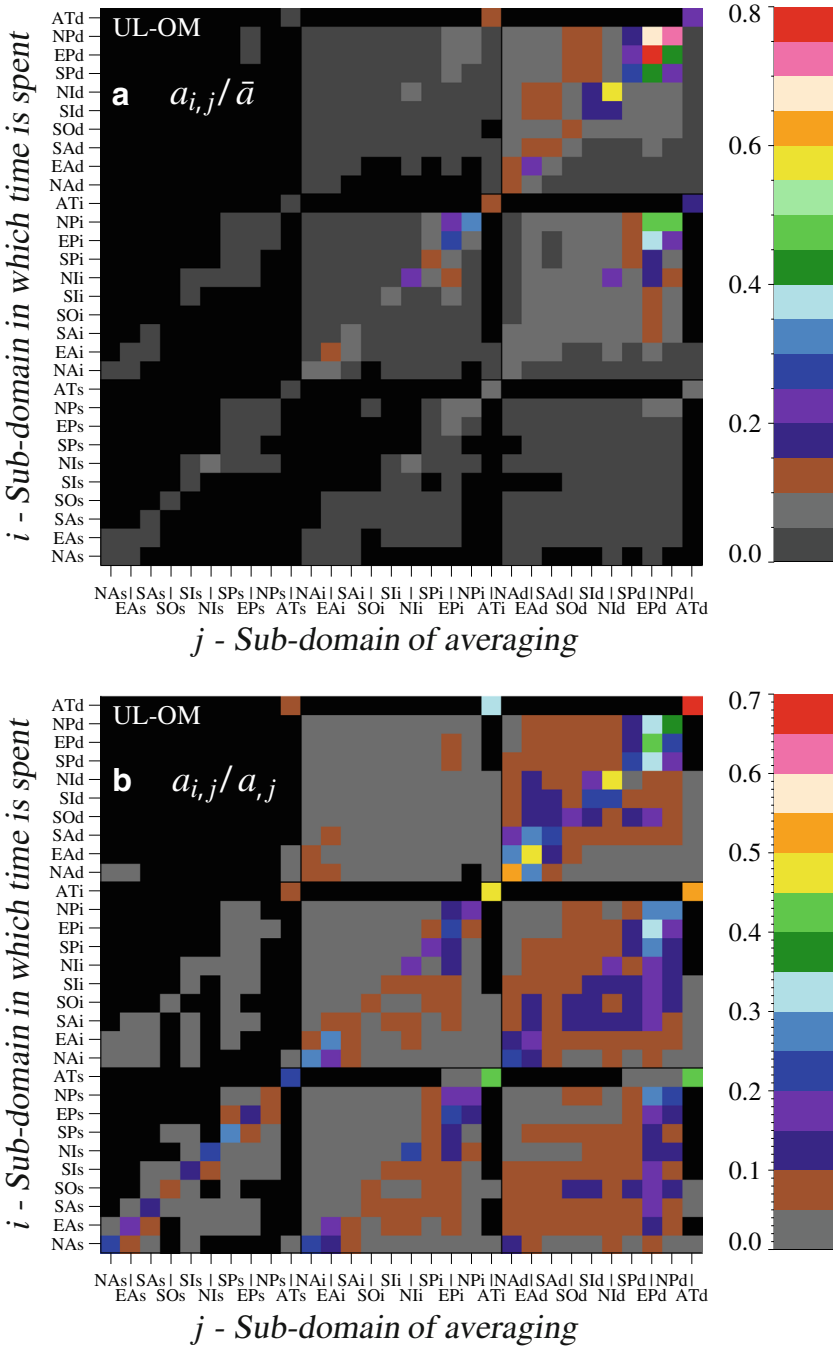

Fig. 9 Partial ages $a_{i,j}$ in the World Ocean normalized by the global average (total) water age $\bar{a}$ = 764 years (**a**, *top panel*) or by the mean (total) water age in the corresponding sub-domain (**b**, *bottom panel*). In both figures, values smaller than 0.0001 are painted in *black*

and the connectivity between the different sub-basins. The information can also be useful to compare different models. We defer to further specific studies the complete exploitation of the partial ages.

7 Conclusion

The concept of age, defined as the time elapsed since a given origin, is widely used to diagnose transport processes in the environment. The age focuses only on the time needed to reach a given location and disregards other aspects of the path followed by the tracer parcel. In this context, the concept of partial age provides a valuable extension of the concept of age. The partial age with respect to a subdomain ω_i is defined as the time spent in ω_i from the same origin used to define the usual age. Partial ages help therefore to keep track of the regions visited by the tracer parcels along their path from the origin. Partial ages with respect to non-overlapping subdomains of the domain of interest forming a partition of the domain of interest provide a natural decomposition of the age into distinct components.

While the concept of partial age is, a priori, applicable to analyze field data, it is particularly useful to diagnose the dynamics of numerical models. In this context, partial ages can be computed using a straightforward extension of the Constituent oriented Age and Residence Time (CART) theory. The procedure relies on the solution of a differential equation for the so-called partial age concentration, which is very similar to the equation for the age concentration introduced in CART for computing the usual (mean) age.

While the concepts and computation procedure look similar to the ones used for the usual age, partial ages provide independent diagnostics, which can be used to gain deeper insights into transport routes and transport rates. In particular, the concentration distribution function c and the newly introduced partial concentration distribution function c_i are independent from each other and convey different information.

The aim of this paper was merely to introduce the concept of partial age, though three illustrations have been discussed. We showed how the concept of partial age can be used to understand and describe the delay introduce by a lateral storage zone in a 1D model. The analysis of the 1D advection-diffusion equation showed that the particles found at some location downstream a source have spent the same amount of time upstream the source than the time spent downstream by the particles found upstream the source at the mirror location. Partial ages also allow a detailed understanding of the transport routes from the ocean's surface to deeper layers. Detailed applications of the concept of partial age are deferred to further studies but the applications discussed above demonstrate the versatility of the concept age and the kind of information that can be gained with it.

Acknowledgments Éric Deleersnijder and Éric J.M. Delhez are both honorary research associates with the Belgian Fund for Scientific Research (F.R.S.-FNRS).

This work was supported by the Fondation BNP Paribas through the project FATES (FAst Climate Changes, New Tools To Understand And Simulate The Evolution of The Earth System) in the scope of its *Climate Initiative* programme.

Appendix A: Partial ages at the origin in a one-dimensional flow

The Lagrangian explanation presented in Section 5 can be further elaborated to compute the partial ages at the origin.

Consider again $2n$-step loops around the origin. As stated above, all such paths share the same probability.

$$\mathcal{P}_{n,n} = p_+^n p_-^n \tag{A.1}$$

The number of paths visiting only the positive half-space $x \geq 0$ is given by the nth Catalan number

$$C_n = \frac{1}{n+1} C_n^{2n} \qquad \text{where} \qquad C_n^{2n} = \frac{(2n)!}{n!\, n!} \tag{A.2}$$

Catalan numbers are usually associated with the number of monotonic paths from the bottom left to the upper right corner of a $n \times n$ grid that may touch but not go above the diagonal of the grid. The paths are monotonic since the only possible moves are upward or to the right. This problem is identical to the one considered here if upward moves are replaced by moves to the right.

Monotonic paths on the $n \times n$ grid can be characterized by their "exceedance," i.e., the number of vertical edges which lie above the diagonal. It can be shown that the set of all monotonic paths can be split into $n+1$ equally sized classes, corresponding to the possible exceedances between 0 and n (Rukavicka 2011).

In CART parlance, this means that all the $2n$ step paths on the 1D lattice can be split into $n+1$ equally sized classes, corresponding to the possible values $0, 2, \ldots, 2(n-1)$ and $2n$ of the two discrete partial ages $\tilde{a}_-$ and $\tilde{a}_+$, where the discrete total age and partial ages are measured in units of the time increment δt. In other words, among the C_n^{2n} possible $2n$-step loops on the 1D lattice, the number of paths giving the particle a discrete partial age $\tilde{a}_+ = 2k$ with $k \in \{0, 1, \ldots, n\}$ is

$$f_{2k}^+(0, 2n) = C_n \tag{A.3}$$

where $f_i^+(M, N)$ denotes the number of paths going from $x_0 = 0$ to $x_M = M\Delta x$ in exactly N steps with a discrete partial age $\tilde{a}_+ = i$. By the same token, one has

$$f_{2k}^-(0, 2n) = C_n \tag{A.4}$$

where $f_i^-(m, N)$ denotes the number of paths going from $x_0 = 0$ to x_M in exactly N steps with a partial age $\tilde{a}_- = i$. The distribution of partial ages among the particles returning to the origin after a $2n$-step loop is uniform.

The mean discrete partial age $\tilde{a}_+$ of these particles is therefore given by

$$\tilde{a}_+(0, 2n) = \frac{\sum_{k=0}^{n} (2k) f_{2k}^+(0, 2n) \mathcal{P}_{n,n}}{\sum_{k=0}^{n} f_{2k}^+(0, 2n) \mathcal{P}_{n,n}} = \frac{2}{n+1} \sum_{k=0}^{n} k = n \tag{A.5}$$

and, similarly, their mean discrete partial age $\tilde{a}_-$ is

$$\tilde{a}_-(0, 2n) = \frac{\sum_{k=0}^{n} (2k) f_{2k}^-(0, 2n) \mathcal{P}_{n,n}}{\sum_{k=0}^{n} f_{2k}^-(0, 2n) \mathcal{P}_{n,n}} = n \tag{A.6}$$

The two mean discrete partial ages of the particle returning to $x = 0$ after a $2n$-step path are equal to each other: half of the steps are taken in $x \leq 0$ and the other half in $x \geq 0$.

As particles are released continuously, the particles found at $x = 0$ have moved along loops around the origin of various lengths, i.e., they are characterized by a wide range of (total) ages. At steady state, their mean (total) discrete age can be computed as the weighted average

$$\tilde{a}(0) = \frac{\sum_{n=0}^{\infty} (2n) C_n^{2n} \mathcal{P}_{n,n}}{\sum_{n=0}^{\infty} C_n^{2n} \mathcal{P}_{n,n}} \tag{A.7}$$

By the generalized binomial theorem, one has

$$\sum_{n=0}^{\infty} C_n^{2n} \mathcal{P}_{n,n} = \sum_{n=0}^{\infty} \frac{(2n)! p_+^n p_-^n}{n!n!} = \frac{1}{\sqrt{1 - 4p_+p_-}} \tag{A.8}$$

and

$$\sum_{n=0}^{\infty} n C_n^{2n} \mathcal{P}_{n,n} = \sum_{n=0}^{\infty} \frac{n(2n)! p_+^n p_-^n}{n!n!} = \frac{2p_+p_-}{(1 - 4p_+p_-)^{3/2}} \tag{A.9}$$

provided that $p_+p_- < 1/4$, i.e. $p_+ \neq p_-$. Therefore,

$$\tilde{a}(0) = \frac{4p_+p_-}{1 - 4p_+p_-} \tag{A.10}$$

The continuous age $a(0)$ can be recovered by taking the limit

$$a(0) = \lim_{\epsilon \to 0} \frac{\epsilon^2}{2\kappa} \tilde{a}(0) \tag{A.11}$$

where

$$p_+ - p_- = \frac{u\,\epsilon}{2\kappa}, \qquad p_+ + p_- = 1 \tag{A.12}$$

One gets therefore

$$a(0) = \frac{2\kappa}{u^2} \tag{A.13}$$

By the above reasoning, since the mean discrete partial ages of the particles found at the origin are half of their total discrete age, whatever the total discrete age, one gets

$$a_-(0) = a_+(0) = \frac{\kappa}{u^2} \tag{A.14}$$

Appendix B: Symmetry of partial ages in a one-dimensional flow

Consider first the partial ages of the particles reaching $x^\star = m\Delta x$ after an N-step path (where $N \geq m$ steps). All the trajectories of these particles comprise $(N + m)/2$ positive steps and $(N - m)/2$ negative steps, in varying orders. Assuming that the steps are independent and that the probabilities p_+ and p_- are constant on the 1D lattice, all these trajectories have the same probability

$$\mathcal{P}(m, N) = p_+^m (p_+p_-)^{(N-m)/2} \tag{B.1}$$

As in Appendix A, let $f_i^+(m, N)$ be the number of possible trajectories running from $x = 0$ to $x^\star$ in exactly N steps with a discrete partial age $\tilde{a}^+ = i$. Assessing the value of f_i^+ is a purely combinatorial problem (closely related to Catalan numbers); f_i^+ does not depend on p and q.

The probability that a particle ends up at $x^\star$ after a N-step path can be expressed as

$$\begin{aligned} P(m, N) &= \sum_{i=0}^{N} f_i^+(m, N) \mathcal{P}(m, N) \\ &= \mathcal{P}(m, N) \sum_{i=0}^{N} f_i^+(m, N) \end{aligned} \tag{B.2}$$

Therefore, the distribution of the discrete partial age $\tilde{a}_+$ of the particles reaching $x^\star$ after an N-step path can be described by

$$\tilde{c}_{+,i}(m, N) = \frac{f_i^+(m, N)\mathcal{P}(m, N)}{\sum_{j=0}^{N} f_j^+(m, N)\mathcal{P}(m, N)} = \frac{f_i^+(m, N)}{\sum_{j=0}^{N} f_j^+(m, N)} \tag{B.3}$$

where $\tilde{c}_{+,i}(m, N)$ is the proportion of particles with a partial age $\tilde{a}_+ = i$ among the particles reaching $x^\star$ after a N-step path. Similarly, one has

$$\tilde{c}_{-,i}(m, N) = \frac{f_i^-(m, N)\mathcal{P}(m, N)}{\sum_{j=0}^{N} f_j^-(m, N)\mathcal{P}(m, N)} = \frac{f_i^-(m, N)}{\sum_{j=0}^{N} f_j^-(m, N)} \tag{B.4}$$

where $\tilde{c}_{-,i}(m, N)$ is the proportion of particles with a partial age $\tilde{a}_- = i$ among the particles reaching $x^\star$ after a N-step path.

Now, by symmetry,

$$f_i^+(m, N) = f_i^-(-m, N) \tag{B.5}$$

since each N-step path from $x = 0$ to $x = m\Delta x$ with i steps taken in the positive half space can be associated with its mirror trajectory going from $x = 0$ to $x = -m\Delta x$ with i steps in the negative half space. The two corresponding trajectories are simply obtained by reversing the direction of every steps.

Injecting (B.5) in (B.3)–(B.4), one gets

$$\tilde{c}_{+,i}(m, N) = \tilde{c}_{-,i}(-m, N) \tag{B.6}$$

which is the main result explaining the symmetry properties of partial ages. In particular, the mean partial ages $\tilde{a}_+(m, N)$

and $\tilde{a}_-(m,N)$ of the particles after N-step paths verify

$$\tilde{a}_+(m,N) = \sum_{i=0}^{N} i\ c_{+,i}(m,N) = \sum_{i=0}^{N} i\ c_{-,i}(-m,N) = \tilde{a}_-(-m,N) \tag{B.7}$$

At steady state, the discrete partial ages for to a continuous release from a point source at the origin are given by

$$\tilde{a}_+^{\infty}(m) = \frac{\sum_{N=m}^{\infty} P(m,N)\,\tilde{a}_+(m,N)}{\sum_{N=m}^{\infty} P(m,N)} \tag{B.8}$$

$$\tilde{a}_-^{\infty}(m) = \frac{\sum_{N=m}^{\infty} P(m,N)\,\tilde{a}_-(m,N)}{\sum_{N=m}^{\infty} P(m,N)} \tag{B.9}$$

From (B.1), one has

$$\mathcal{P}(m,N) = \left(\frac{p_+}{p_-}\right)^m \mathcal{P}(-m,N) \tag{B.10}$$

and, using (B.5),

$$P(m,N) = \left(\frac{p_+}{p_-}\right)^m P(-m,N) \tag{B.11}$$

Using this result together with (B.7), one gets

$$\tilde{a}_+^{\infty}(m) = \tilde{a}_-^{\infty}(-m) \tag{B.12}$$

since the $(p_+/p_-)^m$ factors cancel out.

Appendix C: Partial ages in the great conveyor belt model

The steady state distributions of the age and partial ages in the 1D model schematized in Fig. 4 can be obtained analytically. They are most easily expressed in terms of the non-dimensional coordinate and parameter

$$\xi = \frac{x}{L}, \qquad Pe = \frac{uL}{\kappa} \tag{C.1}$$

The mean age is

$$a = \frac{L}{u}\left[\xi - \frac{e^{Pe\xi}-1}{e^{Pe}-1}\right] \tag{C.2}$$

while the partial ages are given by

$$a_1 = \frac{L}{u}\begin{cases} \xi + \dfrac{1-\mu Pe - e^{Pe(1-\mu)}}{Pe(e^{Pe}-1)}(e^{Pe\xi}-1) & 0 \le \xi \le \mu \\ \dfrac{-1+\mu Pe + e^{-Pe\mu}}{Pe(e^{Pe}-1)}(e^{Pe}-e^{Pe\xi}) & \mu \le \xi \le 1 \end{cases} \tag{C.3}$$

$$a_2 = \frac{L}{u}\begin{cases} \dfrac{-Pe+2\mu Pe - e^{Pe\xi}+e^{Pe(1-\mu)}}{Pe(e^{Pe}-1)}(e^{Pe\xi}-1) & 0 \le \xi \le \mu \\ \xi + \dfrac{1-Pe+\mu Pe - e^{Pe\mu}}{Pe(e^{Pe}-1)}(e^{Pe\xi}-1) & \\ \quad + \dfrac{1-\mu Pe - e^{-Pe\mu}}{Pe(e^{Pe}-1)}(e^{Pe}-e^{Pe\xi}) & \mu \le \xi \le 1-\mu \\ \dfrac{Pe-2\mu Pe - e^{-Pe\mu}+e^{-Pe(1-\mu)}}{Pe(e^{Pe-1}-1)}(e^{Pe}-e^{Pe\xi}) & 1-\mu \le \xi \le 1 \end{cases} \tag{C.4}$$

$$a_3 = \frac{L}{u}\begin{cases} \dfrac{-1-\mu Pe + e^{Pe\mu}}{Pe(e^{Pe}-1)}(e^{Pe\xi}-1) & 0 \le \xi \le 1-\mu \\ -1+\xi + \dfrac{1+\mu Pe - e^{-Pe(1-\mu)}}{Pe(e^{Pe}-1)}(e^{Pe}-e^{Pe\xi}) & 1-\mu \le \xi \le 1 \end{cases} \tag{C.5}$$

One can verify that

$$a = a_1 + a_2 + a_3 \tag{C.6}$$

Appendix D: Location of the maximum of the partial age

In this appendix, we show that the absolute maximum of the steady-state spatial distribution of the partial age a_i can only occur on the boundary or in the interior of the corresponding subdomain ω_i.

The steady-state distribution of a_i can be obtained as the solution of the differential problem

$$\begin{cases} \nabla\cdot(\mathrm{K}\cdot\nabla a_i - a_i\mathbf{v}) + \delta_{\omega_i} = 0 & \forall \mathrm{x} \in \omega \\ a_i(\mathrm{x}) = 0 & \forall \mathrm{x} \in \Gamma_s \\ [\mathrm{K}\cdot\nabla a_i(\mathrm{x})]\cdot\mathrm{n} = 0 & \forall \mathrm{x} \in \Gamma_i \end{cases} \tag{D.1}$$

where $\mathbf{v}$ is the velocity vector, K is the diffusion tensor, ω is the model domain, Γ_s is the ocean surface where the age is set to zero, $\Gamma_i = \partial\omega\backslash\Gamma_s$, and n is the outer unit normal to Γ_i. The boundary Γ_i is assumed to be impermeable, i.e.,

$$\mathbf{v}\cdot\mathbf{n} = 0 \qquad \forall x \in \Gamma_i \tag{D.2}$$

Let a_i^{max} denote the maximum value of a_i in ω_i and introduce the age difference

$$\hat{a}_i(\mathrm{x}) \equiv a_i(\mathrm{x}) - a_i^{max} \tag{D.3}$$

This difference satisfies the differential equation

$$\nabla\cdot(\mathrm{K}\cdot\nabla\hat{a}_i - \hat{a}_i\mathrm{v}) + \delta_{\omega_i} = 0 \qquad \forall \mathrm{x} \in \omega \tag{D.4}$$

and the boundary conditions

$$\begin{cases} \hat{a}_i(\mathrm{x}) = -a_i^{max} & \forall \mathrm{x} \in \Gamma_s \\ \left[\mathrm{K}\cdot\nabla\hat{a}_i(\mathrm{x})\right]\cdot\mathrm{n} = 0 & \forall \mathrm{x} \in \Gamma_i \end{cases} \tag{D.5}$$

With these equations, we show below that the positive part

$$\hat{a}_{i,+}(\mathrm{x}) = \frac{\hat{a}_i(\mathrm{x}) + |\hat{a}_i(\mathrm{x})|}{2} \tag{D.6}$$

of $\hat{a}_i$ is zero everywhere in ω.

From the definition (D.3), it is clear that $\hat{a}_i$ takes only negative values in ω_i so that

$$\hat{a}_{i,+}(\mathrm{x}) = 0 \qquad \forall \mathrm{x} \in \omega_i \tag{D.7}$$

Also, from (D.5), one can conclude that

$$\hat{a}_{i,+}(\mathrm{x}) = 0 \qquad \forall \mathrm{x} \in \Gamma_s \tag{D.8}$$

To show that $\hat{a}_{i,+}$ also vanishes in the whole model domain ω, we first multiply (D.4) by $\hat{a}_{i,+}$, integrate over the model domain ω and re-write the equation as (See Lewandowski (1997) for technical details)

$$\int_\omega \left[\nabla\cdot\left(\hat{a}_{i,+}\mathrm{K}\cdot\nabla\hat{a}_i\right) - \nabla\hat{a}_{i,+}\cdot\mathrm{K}\cdot\nabla\hat{a}_i - \hat{a}_{i,+}\nabla\cdot\left(\hat{a}_i\mathrm{v}\right) + \hat{a}_{i,+}\delta_{\omega_i}\right] dV = 0 \tag{D.9}$$

Since the negative part of $\hat{a}_i$ vanishes where $\hat{a}_{i,+}$ differs from zero and since the flow field is divergence free, one has

$$\int_\omega \left[\nabla\cdot\left(\hat{a}_{i,+}\mathrm{K}\cdot\nabla\hat{a}_{i,+}\right) - \nabla\hat{a}_{i,+}\cdot\mathrm{K}\cdot\nabla\hat{a}_{i,+} - \frac{1}{2}\nabla\cdot\left(\hat{a}_{i,+}^2\mathrm{v}\right) + \hat{a}_{i,+}\delta_{\omega_i}\right] dV = 0 \tag{D.10}$$

Using the divergence theorem and taking into account the boundary conditions (D.5) and (D.8), the integral of the first term of (D.10) on ω can be shown to vanish, i.e.,

$$\int_\omega \nabla\cdot\left(\hat{a}_{i,+}\mathrm{K}\cdot\nabla\hat{a}_{i,+}\right)dV = \int_{\partial\omega}\left(\hat{a}_{i,+}\mathrm{K}\cdot\nabla\hat{a}_{i,+}\right)\cdot\mathrm{n}\, d\sigma = 0 \tag{D.11}$$

Similarly, using (D.2) and (D.8), one has

$$\int_\omega \nabla\cdot\left(\hat{a}_{i,+}^2\mathrm{v}\right) dV = \int_{\omega_i}\hat{a}_{i,+}^2\mathrm{v}\cdot\mathrm{n}\, d\sigma = 0 \tag{D.12}$$

and

$$\int_\omega \hat{a}_{i,+}\delta_{\omega_i}\, dV = \int_{\omega_i}\hat{a}_{i,+}\, dV = 0 \tag{D.13}$$

since, by (D.7), $\hat{a}_{i,+}$ is zero on ω_i. On integrating (D.10) on ω, one gets therefore

$$\int_\omega \nabla\hat{a}_{i,+}\cdot\mathrm{K}\cdot\nabla\hat{a}_{i,+}dV = \int_{\omega\backslash\omega_i}\nabla\hat{a}_{i,+}\cdot\mathrm{K}\cdot\nabla\hat{a}_{i,+}dV = 0 \tag{D.14}$$

If the diffusion tensor K is assumed positive definite, as it must be from a physical point of view, one can conclude that

$$\nabla\hat{a}_{i,+} = 0, \qquad \forall \mathrm{x} \in \omega\backslash\omega_i \tag{D.15}$$

Since $\hat{a}_{i,+}$ vanishes on Γ_s and $\partial\omega_i$, this further implies that

$$\hat{a}_{i,+} = 0, \qquad \forall \mathrm{x} \in \omega\backslash\omega_i \tag{D.16}$$

(if the model domain is a connected set) and

$$a_i(\mathrm{x}) \le a_i^{max} \qquad \forall \mathrm{x} \in \omega \tag{D.17}$$

The maximum value of a_i on ω_i is also the maximum value on the whole model domain ω. The inequality does not preclude that the maximum value a_i^{max} can also be reached in $\omega\backslash\omega_i$, but it cannot be exceeded.

The above result (D.17) is obtained with rather general hypotheses about the flow, the parameterization of diffusion, and the model domain. It is therefore rather general.

The hypothesis of a steady state flow is, however, essential and cannot be dispensed with. It is indeed not difficult to design an unsteady flow for which (D.17) does not hold. A simple such exemple is proposed in Fig. 10 where we

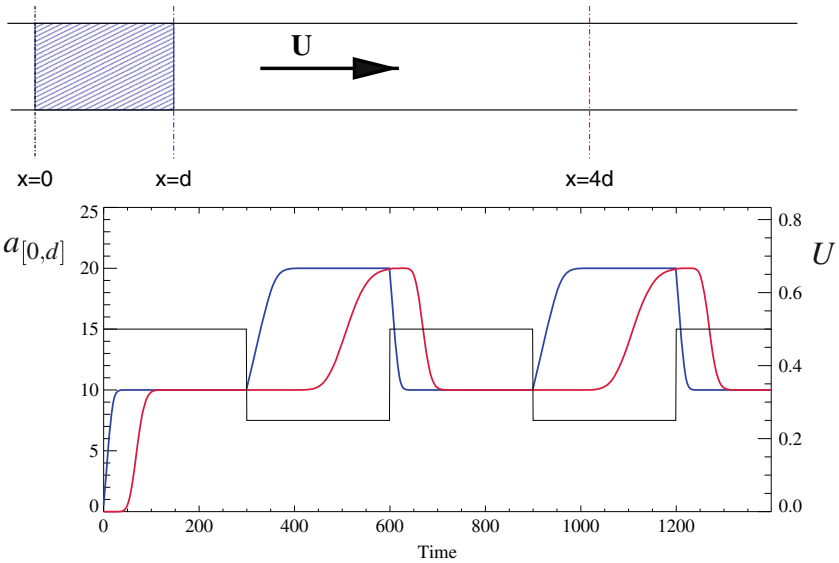

Fig. 10 Partial age in the 1D periodic (advection dominated) flow schematized in the top panel. The temporal evolution of $a_{[0,d]}$ is shown in the *bottom* panel for $x = d$ (*blue*) and $x = 4d$ (*red*). When the velocity (*thin black*, right axis) suddenly increases, e.g., at time $t = 600$ s, $a_{[0,d]}$ is larger at $x = 4d$ than at $x = d$

consider a 1D periodic (advection dominated) flow. The boundary condition imposes ages to be zero at $x = 0$. The partial age $a_{[0,d]}$ is computed with respect to the region $[0, d]$ (hatched area in Fig. 10). When the velocity increases, the partial age downstream of $[0, d]$, carries the signature of a lower velocity. Therefore, during a while $a_{[0,d]}$ downstream exhibits larger values than the one observed at the exit of the segment.

References

Beckers JM, Delhez E, Deleersnijder E (2001) Some properties of generalized age-distribution equations in fluid dynamics. SIAM J Appl Math 61:1526–1544

Bencala K, Walters R (1983) Simulation of solute transport in a mountain pool-and-riffle stream: a transient storage model. Water Resour Res 19(3):718–724

Bendtsen J, Hansen JL (2013) A model of life cycle, connectivity and population stability of benthic macro-invertebrates in the North Sea/Baltic Sea transition zone. Ecol Model 267:54–65

Bendtsen J, Gustafsson KE, Soderkvist J, Hansen JLS (2009) Ventilation of bottom water in the North Sea-Baltic Sea transition zone. J Mar Syst 75:138–149

Bolin B, Rodhe H (1973) A note on the concepts of age distribution and residence time in natural reservoirs. Tellus 25:58–62

Campin J-M, Goosse H (1999) Parameterization of density-driven downsloping flow for a coarse-resolution ocean model in z-coordinate. Tellus 51:421–430

Campin J-M, Fichefet T, Duplessy J-C (1999) Problems with using radiocarbon to infer ocean ventilation rates for past and present climates. Earth Planet Sci Lett 16(1):17–24

Chen X (2007) A laterally averaged two-dimensional trajectory model for estimating transport time scales in the Alafia River estuary, Florida. Hydrodynamic Control Aquat Ecosyst Process 75(3):358–370

Cornaton F (2012) Transient water age distributions in environmental flow systems: the time-marching Laplace transform solution technique. Water Resour. Res 48:W03524

de Brye B, de Brauwere A, Gourgue O, Delhez EJM, Deleersnijder E (2012) Water renewal timescales in the Scheldt Estuary. J Mar Syst 94:74–86

Deleersnijder E (2015) Can CART's classical age distribution function be derived from partial age distribution function? Working paper available at http://hdl.handle.net/2078.1/162261, p 17

Deleersnijder E, Campin J-M (1995) On the computation of the barotropic mode of free-surface world ocean model. Ann Geophys 13:675–688

Deleersnijder E, Delhez EJM (2004) Symmetry and asymmetry of water ages in a one-dimensional flow. J Mar Syst 48:61–66

Deleersnijder E, Campin JM, Delhez EJM (2001) The concept of age in marine modelling I. Theory and preliminary model results. J Mar Syst 28:229–267

Deleersnijder E, Delhez EJM, Crucifix M, Beckers JM (2001) On the symmetry of the age field of a passive tracer released into a one-dimensional fluid flow by a point source. Bull Soc R Sci Liége 70:5–21

Deleersnijder E, Mouchet A, Delhez EJM, Beckers JM (2002) Transient behaviour of water ages in the World Ocean. Math Comput Model 36:121–127

Deleersnijder E, Mouchet A, de Brauwere A, Delhez EJM, Hanert E (2014) The concept of partial age, a generalisation of the notion of age: theory, idealised illustrations and realistic applications. JONSMOD 2014 Workshop (Brussels, 12-14 May 2014), available on the web at http://hdl.handle.net/2078.1/153807 or https://publicwiki.deltares.nl/display/JONSMOD/Presentations+2014

Delhez EJM, Deleersnijder E (2002) The concept of age in marine modelling II. Concentration distribution function in the English Channel and the North Sea. J Mar Syst 31:279–297

Delhez EJM, Campin J-M, Hirst AC, Deleersnijder E (1999) Toward a general theory of the age in ocean modelling. Ocean Model 1:17–27

Delhez EJM, Lacroix G, Deleersnijder E (2004) The age as a diagnostic of the dynamics of marine ecosystem models. Ocean Dyn 54:221–231

DeVries T, Primeau F (2010) An improved method for estimating water-mass ventilation age from radiocarbon data. Earth Planet Sci Lett 295:367–378

Du J, Shen J (2015) Decoupling the influence of biological and physical processes on the dissolved oxygen in the Chesapeake Bay. J Geophys Res Oceans 120(1):78–93

England MH (1995) The age of water and ventilation timescales in a global ocean model. J Phys Oceanogr 25:2756–2777

England MH, Maier-Reimer E (2001) Using chemical tracers to assess ocean models. Rev Geophys 39(1):29–70

Ginn TR (1999) On the distribution of multicomponent mixtures over generalized exposure time in subsurface flow and reactive transport: foundations, and formulations for groundwater age, chemical heterogeneity, and biodegradation. Water Resour Res 35(5):1395–1407

Gnanadesikan A, Russell JL, Zeng F (2007) How does ocean ventilation change under global warming? Ocean Sci 3(1):43–53

Goode DJ (1996) Direct simulation of groundwater age. Water Resour Res 32:289–296

Gourgue O, Deleersnijder E, White L (2007) Toward a generic method for studying water renewal, with application to the epilimnion of Lake Tanganyika. Estuar Coast Shelf Sci 74:628–640

Haine TWN, Hall TM (2002) a generalized transport theory: water-mass composition and age. J Phys Oceanogr 32:1932–1946

Hall TM, Haine TWN (2004) Tracer age symmetry in advective-diffusive flows. J Mar Syst 48:51–59

Hall TM, Plumb RA (1994) Age as a diagnostic of stratospheric transport. J Geophys Res-Atmos 99:1059–1070

Holzer M, Hall TM (2000) Transit-time and tracer-age distributions in geophysical flows. J Atmos Sci 57:3539–3558

Khatiwala S, Primeau F, Hall T (2009) Reconstruction of the history of anthropogenic CO_2 concentrations in the ocean. Nature 462(7271):346–349

Kumar A, Dalal D (2010) Analysis of solute transport in rivers with transient storage and lateral inflow: an analytical study. Acta Geophysica 58(6):1094–1114

Lewandowski R (1997) Analyse mathématique et océnographie, masson Edition. No. 39 in Recherches en mathématiques appliquées. Paris

Liu Z, Wang H, Guo X, Wang Q, Gao H (2012) The age of Yellow River water in the Bohai Sea. J Geophys Res Oceans 117(C11):C11006

Meier HEM (2007) Modeling the pathways and ages of inflowing salt- and freshwater in the Baltic Sea. Estuar Coast Shelf Sci 74:610–627

Mercier C, Delhez EJM (2007) Diagnosis of the sediment transport in the Belgian Coastal Zone. Estuar Coast Shelf Sci 74:670–683

Munk W (1966) Abyssal recipes. Deep Sea Res Oceanogr Abstr 13:707–730

Plus M, Dumas F, Stanisiére J-Y, Maurer D (2009) Hydrodynamic characterization of the Arcachon Bay, using model-derived descriptors. 100 Years of Research within the Bay of Biscay XI International Symposium on Oceanography of the Bay of Biscay 29(8):1008–1013

Primeau F (2005) Characterizing transport between the surface mixed layer and the ocean interior with a forward and adjoint global ocean transport model. J Phys Oceanogr 35:545–564

Ren Y, Lin B, Sun J, Pan S (2014) Predicting water age distribution in the Pearl River Estuary using a three-dimensional model. J Mar Syst 139(0):276–287

Rukavicka J (2011) On generalized Dyck paths. Electron J Comb 18(1):P40

Runkel R, Chapra S (1993) An efficient numerical solution of the transient storage equations for solute transport in small streams. Water Resour Res 29(1):211–215

Shaffer G, Sarmiento J (1995) Biogeochemical cycling in the global ocean: 1. a new, analytical model with continuous vertical resolution and high-latitude dynamics. J Geophys Res 100:2659–2672

Takeoka H (1984) Fundamental concepts of exchange and transport time scales in a coastal sea. Cont Shelf Res 3:311–326

Thiele G, Sarmiento J (1990) Tracer dating and ocean ventilation. J Geophys Res 95(C6):9377–9391

Villa M, Lopez-Gutierrez J, Suh K-S, Min B-I, Periañez R (2015) The behaviour of 129i released from nuclear fuel reprocessing factories in the North Atlantic Ocean and transport to the Arctic assessed from numerical modelling. Mar Pollut Bull 90:15–24

Wagner B, Harvey J (1997) Experimental design for estimating parameters of rate-limited mass transfer: analysis of stream tracer studies. Water Resour Res 32(8):2441–2451

Zimmerman JTF (1976) Mixing and flushing of tidal embayments in the western Dutch Wadden Sea. Part I: Distribution of salinity and calculation of mixing time scales. Neth J Sea Res 10:149–191